Article

Effect of Nano-Bubble Irrigation on the Yield and Greenhouse Gas Warming Potential of Greenhouse Tomatoes

Hongjun Lei [ID], Wenbo Wang, Yuqi Liang, Zheyuan Xiao [ID], Hongwei Pan *, Luyang Wang and Mengyuan Du

School of Water Conservancy, North China University of Water Resources and Electric Power, Zhengzhou 450046, China; leihongjun@ncwu.edu.cn (H.L.); x20211010054@stu.ncwu.edu.cn (W.W.); z202210010109@stu.ncwu.edu.cn (Y.L.); x201810102054@stu.ncwu.edu.cn (Z.X.); 13361070901@163.com (L.W.); 201705812@stu.ncwu.edu.cn (M.D.)
* Correspondence: phw103@163.com; Tel.: +86-155-1615-1051

Abstract: Nano-bubble irrigation, as a new irrigation technology, can deliver fertilizer-mixed oxygen-enriched water to the root zone of crops, representing a new means for increasing crop yield and carbon sequestration and emission reduction. To systematically analyze the effects of nano-bubble irrigation on crop yield, soil aeration, and soil greenhouse gas (GHG) emissions, as well as evaluating its contribution to the net greenhouse warming potential (*NGWP*) in greenhouse agriculture, this study was conducted in greenhouse facilities in Zhengzhou, China and focused on tomato plants. A 2-factor, 2-level, completely randomized trial of nitrogen application (low N_1: 120 kg/hm^2 and normal N_2: 180 kg/hm^2), conventional irrigation, and nano-bubble irrigation (C: 5 ppm and A: 15 ppm) was conducted. Compared with conventional irrigation, crop yield increased by 18.94% and 16.36% ($p < 0.05$), CO_2 emission by 10.72% and 5.71% ($p < 0.05$), N_2O emission by 29.76% and 35.74% ($p < 0.05$), and CH_4 uptake by 300.67% and 327.67% ($p < 0.05$) under nano-bubble irrigation. The nano-bubble irrigation increased the crop yield, thus significantly improving the NGWP sink for greenhouse gases. The low-nitrogen and regular-nitrogen treatments increased NGWP by 22.69% and 14.52%, respectively ($p < 0.05$). This suggests that nano-bubble irrigation can significantly improve soil aeration, increase tomato yield and biomass, and significantly improve crop carbon sequestration. In the future, nano-bubble irrigation can be used along with soil amendments to achieve a more efficient increase in yield and enhance the ability of farmland to sequester carbon and reduce emissions.

Keywords: nano-bubble irrigation; greenhouse gas; soil aeration; fertilizer use efficiency; carbon sequestration and emission reduction

1. Introduction

Emissions of greenhouse gases (GHGs) including N_2O, CO_2, and CH_4 are the key factors causing global warming. Direct GHG emissions from agriculture have contributed to approximately 12% of the total in global GHG emissions [1]. China is a large agricultural country with a greenhouse gas production scale that also quite large, and is one of the largest greenhouse gas emitters in the world. Agricultural ecosystems play a significant role in the emission of greenhouse gases and also serve as a crucial component of the carbon sequestration system. These ecosystems possess robust carbon sequestration capabilities [2]. In addition, the farmland management process involves the carbon cycle, which includes the input and output of carbon materials [3]. Chinese tomato planting area and output are at the forefront in the world. It was found that reasonable application of nitrogen fertilizer could improve the yield and quality of tomato, but excessive application of nitrogen fertilizer would lead to a decrease in yield and quality of tomato [4]. In addition, the nitrogen form and ratio had significant effects on the growth, yield and quality of tomato. The combined application of organic fertilizer and chemical fertilizer can significantly improve the yield and quality of tomato [5]. However, conventional subsurface drip

irrigation may negatively impact the growth of tomatoes to varying degrees due to root hypoxia [6,7].

Nano-bubble irrigation is a new type of water-saving irrigation measure further developed on the basis of subsurface drip irrigation, in which oxygen-enriched water is mixed with fertilizers and delivered to the root zone of crops [8]. It offers a new way to increase crop yields, sequester carbon, and reduce emissions. The optimal management of nitrogen fertilizer in regulated deficit irrigation has a high effect on crop resource utilization efficiency and yield [9]. Currently, scientists are actively exploring greenhouse gas emissions from agroecosystems. Qian et al. reported that future studies need to focus on the uncertainty of GHG emissions assessment, integrated agronomic measures and strategies for emissions reduction, and soil microbial functions [10]. Jin et al. studied the effect on cucumber through greenhouse experiments, and concluded that compared with non-aerated treatment, aeration irrigation could improve the nutrient absorption and utilization rate, thereby releasing the high-yield potential by increasing the aeration morphological index [11]. Chen et al. found that the response of soil CO_2 and N_2O emissions of greenhouse tomatoes to aerated irrigation did not significantly increase the comprehensive greenhouse effect of soil CO_2 and N_2O [12]. Precision irrigation seems to allow simultaneous increases in crop yields and reductions in GHG emissions under warming conditions [13,14]. Shahar B et al. showed that adding gas irrigation can reduce CO_2 emissions, and the result will be increased production regardless of soil type or consumption [15]. Additional research is required to understand the impact of nano-bubble irrigation technology on GHG emissions and its potential for carbon sequestration in greenhouse farmland ecosystems. This research is crucial for mitigating greenhouse effects, reducing agricultural non-point source pollution, and promoting sustainable agricultural development. Furthermore, as China progresses in agricultural modernization, aerated irrigation technology is expected to gain wider usage. Aerated irrigation has been implemented in certain regions such as Xinjiang, Gansu, and Shaanxi. Despite its limited current usage, aerated irrigation technology offers an effective solution for reducing greenhouse gas emissions and plays a crucial role in China's pursuit of low-carbon economic development. Given the ongoing technological advancements and government support, the future prospects for aerated irrigation technology in China are highly promising.

Nano-bubble irrigation technology is a novel agricultural technique that has not been extensively researched in terms of its impact on plant growth and yield. Additionally, there have been limited attempts to explore the combination of nano-bubble irrigation with greenhouse gas warming potential. Investigating the effect of nano-bubble irrigation on greenhouse tomato yield can provide valuable insights into the agricultural production potential of this emerging technology, offering new ideas and approaches to improve crop yield. Understanding the greenhouse gas warming potential is crucial in studying global climate change [16]. Therefore, studying the influence of nano-bubble irrigation on greenhouse gas warming potential is essential for evaluating the environmental impact of this emerging agricultural technology. This research holds great significance in promoting sustainable agricultural development and addressing climate change challenges.

2. Materials and Methods

2.1. Overview of the Experimental Site

The experiment was conducted from 16 March to 11 July 2019 in a greenhouse (34°46′56″ N, 113°47′21″ E) at the Laboratory of Efficient Water Use in Agriculture, North China University of Water Resources and Electric Power, Zhengzhou, China. The average annual temperature of the experimental site was 14.4 °C, and the annual sunshine hours were 2400 h. The greenhouse temperature and humidity dynamics during the reproductive period of tomato are shown in Figure 1.
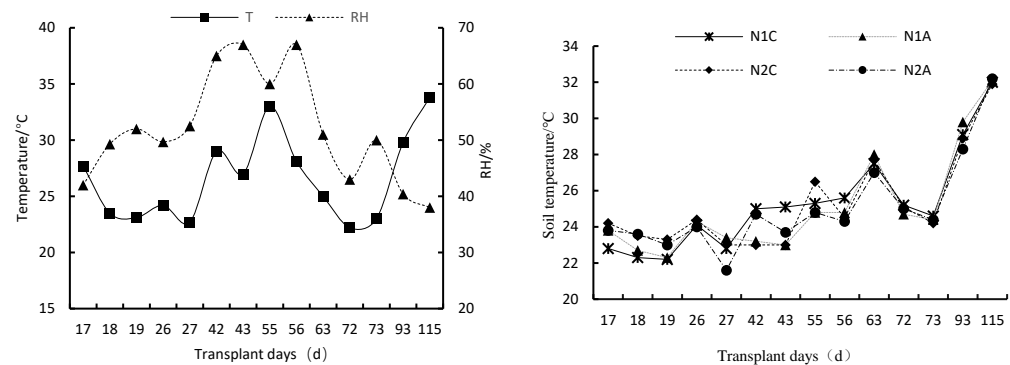
Figure 1. Dynamics of greenhouse temperature (T), relative humidity (RH), and soil tem-perature during the growth period of greenhouse tomatoes.

2.2. Test Materials

Tomato "Fen Ouya" was used as the test variety. Tomatoes were transplanted from 3 leaves and 1 heart to 4 leaves and 1 heart, bottom water was thoroughly poured on the day of transplanting, film was applied 10 days after transplanting, vines were hung when the plant height was 30–40 cm, and three spikes of fruits were topped. According to the growth traits of the crop, the fertility period was divided into four periods: seedling period (*mid-March to early-mid April*), flowering and fruit bearing period (*early-mid April to mid-May*), harvesting period (*mid-May to early-mid June*), and ripening period (*early-mid June to early-mid July*). The total life span of tomato was 115 d. The test soil was Zhengzhou clayey soil.

The test soil was a clay loam in Zhengzhou, with 32.99%, 34.03% and 32.98% of sand (0.02–2 mm), flour (0.002–0.02 mm) and clay (<0.002 mm), respectively. The physical and chemical properties of the 0–40 cm tillage base of the test soil are shown in Table 1.

Table 1. Experimental soil 0–40 cm plough layer basic physical and chemical properties.

Soil Depth	Soil Bulk Density (g·cm^{-3})	Field Water Retention (cm^3·cm^{-3})	Soil Organic Matter (g·kg^{-1})	Total N (g·kg^{-1})	Total P (g·kg^{-1})	Total K (g·kg^{-1})	pH
0–10 cm	1.24						
10–20 cm	1.47						
20–30 cm	1.51	0.28	13.62	0.81	0.79	30.38	6.5
30–40 cm	1.55						

2.3. Experimental Design

The experiment was set up with 2 factors and 2 levels of fertilizer application (N_1, N_2) and dissolved oxygen (C, A) in a fully randomized group design with 4 treatments and 3 applications. The experimental design is listed in Table 2.

Table 2. Experimental design.

Treatment	Nitrogen Application Rate (kg·hm^{-2})	Dissolved Oxygen (ppm)
N_1C	120	5
N_1A	120	15
N_2C	180	5
N_2A	180	15

Note: N_1, N_2 are the low and normal nitrogen application rates. C, A are the non-aerated and continuous aerated treatments.

A total of 12 plots, each 4 m in length and 1 m in width, were planted with 10 tomato plants per plot at 33 cm spacing, and a nano-bubble drip irrigation device was used for aeration, and water transportation was conducted using a non-pressure compensating drip tape with the model JOHNDEERE. The drip tape had a diameter of 16 mm and a wall thickness of 0.6 mm. The drip heads were designed to have a flow rate of 1.2 L/h, with a spacing of 33 cm between them. The drip tape was buried to a depth of approximately 15 cm. The plants were positioned approximately 10 cm away from the drip heads and were cultivated parallel to the drip tape.

2.4. Test Management

The test fertilizers were balanced, and high-potassium water-soluble fertilizers were applied alternately; the mass fractions of balanced water-soluble fertilizers N, P_2O_5 and K_2O were 20%, 20% and 20%, respectively; the mass fractions of high-potassium water-soluble fertilizers N, P_2O_5 and K_2O were 5%, 10% and 40%, respectively; and the mass fractions of Fe, Mn, Zn, Cu, Mo, and B were, respectively, 0.10%, 0.05%, 0.15%, 0.05%, 0.05%, and 0.10%, respectively (Primosol, Kangtuo Fertilizer Co., LTD, Handan, China). No basal fertilizer was applied before tomato transplanting, and a topdressing was applied at 14, 23, 40, 55 and 72 days after transplanting tomatoes at a ratio of 1:1:2:2:2. Water-soluble fertilizer was mixed into the water stream using a fertilizer applicator, and then applied after circulating and mixing in the water storage tank. In the test, water storage lines, circulation pumps, and venturi air injector (Mazzei air injector 684, CA the United States Mazzei Corp, Bakersfield, CA, USA) were used to produce dissolved oxygen of 15 ppm in dissolved oxygen water (aeration for 20 min), through the underground drip irrigation system for irrigation. Each plot had an independent water supply system with a water supply pressure of 0.10 MPa. The amount of irrigation water was measured using a drip meter. Soil substrate potential was measured by a tension meter located 10 cm radially and 20 cm longitudinally from the plant (type 12 split tensiometer, Institute of Agricultural Irrigation (FIRI), Chinese Academy of Agricultural Sciences (CAAS)). Irrigation in the experiment began when the soil substrate potential reached -30 ± 5 kPa. The amount of irrigation water was calculated according to Equation (1) [17].

$$W = A \times E_{pan} \times K_{cp}, \tag{1}$$

where W is the amount of irrigation water (mm); A is the irrigation control area (m^2; 4 m^2 in this experiment); E_{pan} is the evapotranspiration between two irrigation intervals (mm); K_{cp} is the evapotranspiration dish coefficient (in this experiment, the K_{cp} was set at 1.0). The irrigation time and the amount of irrigation water are shown in Table 3.

Table 3. Irrigation volume during crop growing period.

Irrigation Time	Days after Transplanting/days	Daily Average Evapotranspiration mm	Irrigation Water Volume mm	Irrigation Time	Days after Transplanting/days	Daily Average Evapotranspiration mm	Irrigation Water Volume mm
31 March 2019	16	0.703	4.5	26 May 2019	72	2.625	8.4
10 April 2019	26	1.8	7.2	1 June 2019	78	4.75	11.4
16 April 2019	32	3.75	9	9 June 2019	86	3.375	10.8
24 April 2019	40	3	9.6	16 June 2019	93	2.786	7.8
2 May 2019	48	3.094	9.9	26 June 2019	103	2.775	11.1
10 May 2019	56	3.375	10.8	4 July 2019	111	2.625	8.4
18 May 2019	64	3.281	10.5	$\sum$			119.4

2.5. Sample Collection and Measurement Methods

2.5.1. Monitoring of Soil Environmental Indicators

Soil environmental indicators include soil temperature (T), water-filled pore space (WFPS), oxidation reduction potential (E_h), dissolved oxygen (DO), and oxygen diffusion rate (ODR). Soil temperature in the experiment was measured at a depth of 5 cm using a geothermometer; WFPS was measured using a 20 cm buried moisture sensor probe (FDS-100, Handan Qingsheng Electronic Technology Co., Ltd., Handan, China); E_h was measured using a specialized instrument (TR-901, INESA Scientific Instrument Co., Ltd., Shanghai, China); ODR was measured using a fully automatic depolarization method instrument (R-1-034, INESA Scientific Instrument Co., Ltd., Shanghai, China); DO was measured using a fiber optic oxygen measuring instrument connected to an oxygen-sensitive probe (OXY4 mini, Presens, Regensburg, Germany).

2.5.2. Greenhouse Gas Sample Collection and Analysis

Gas samples in the experiment were collected using a static chamber made of cylindrical hollow PVC pipes. The chamber and its base had a wall thickness of 6 mm and an inner diameter of 15 cm. The height of the chamber was 10 cm. In the experiment, two tomato plants were randomly chosen for burying the static chamber bases. Three plots were selected for gas monitoring in each treatment. During burial, half of the chamber base was inserted into the soil. A circular film covered the chamber when no sampling was performed. During sampling, the film was removed, and the chamber was sealed with a rubber ring. In the study, gas collection was carried out at 17, 18, 19, 26, 27, 42, 43, 55, 56, 63, 72, 73, 93, and 115 days after transplantation, the sampling time was at 0, 10, 20, and 30 min after the box was covered, and gas collection was carried out by using a 50 mL syringe with a three-way valve to collect 35 mL of gas at a time, with 5 mL of gas used for rinsing and the remaining 30 mL injected into a 12 mL stoppered sample bottle and stored in a refrigerator at 4 °C. The collected gas samples were analyzed by a gas chromatograph (GC9310, Shanghai Spectrum Instrument Co., Ltd., Shanghai, China) for N_2O, CH_4 and CO_2 concentrations within 14 days. While the gases were collected, the temperature inside the chamber was measured using a thermometer inserted in the chamber. The emission fluxes of N_2O, CH_4 and CO_2 were calculated according to Equation (2) [18,19].

$$F = \rho \cdot h \cdot \frac{273}{273 + T} \cdot \frac{dc}{dt}, \tag{2}$$

where F is the soil GHG emissions flux, mg/(m^2·h); ρ is the gas density in the standard state, $\rho(CO_2) = 1.965$ g/cm^3, $\rho(N_2O) = 1.98$ g/cm^3, $\rho(CH_4) = 0.714$ g/m^3; h is the height of the box, m; dc/dt is the rate of change in gas concentration, mg/(m^3·h); and T is the gas temperature in the box, °C.

Cumulative gas emissions were calculated according to Formula (3).

$$M = \sum_{i=1}^{n} \frac{F_{i+1} + F_i}{2} \cdot (t_{i+1} - t_i) \cdot 24, \tag{3}$$

where M is the cumulative soil gas emissions (N_2O in μg·m^{-2}·h^{-1}, CO_2 in mg·m^{-2}·h^{-1}, and CH_4 in μg·m^{-2}·h^{-1}); F is the gas emission flux, i is the number of times gas emission flux was monitored, $t_{i-1} - t_i$ is the number of consecutive days between the two endpoints of the monitoring interval (d), and n is the total number of times cumulative soil gas emissions was monitored.

2.5.3. Net Primary Productivity (NPP)

Crop net primary productivity (NPP), as a key variable characterizing vegetation vigor, is not only the basis of energy and material flow of organisms, but also relates to the strength of the ecosystem's ability to fix carbon. NPP is measured after crop harvest, which includes crop fruits, above-ground biomass, and below-ground biomass [20].

2.5.4. Evaluation of Net Greenhouse Effect of Farmland Ecosystems

The net greenhouse warming potential (NGWP) of greenhouse farmland is referenced to the crop-based approach (CBA) and the soil and crop-based approach (S&CBA) [21]; it represents the integrated greenhouse effect of greenhouse farmland ecosystems obtained in terms of CO_2 equivalent.

(1)   Crop-based approach, CBA

$$NGWP = GWP_{NBP} - GWP_{GHG_s} - GWP_{indiret}, \tag{4}$$

$$GWP_{NBP} = GWP_{NPP} + GWP_{input} - GWP_{output}, \tag{5}$$

NGWP—Combined greenhouse effect, expressed as CO_2 equivalent (CO_2-eq), kg/hm^2;

GWP_{NBP} [19]—The warming potential of net biota productivity, expressed as CO_2 equivalent (CO_2-eq), kg/hm^2;

GWP_{NPP}—Warming potential of primary productivity, expressed as CO_2 equivalent (CO_2-eq), kg/hm^2;

GWP_{input}—Warming potential of economic yields and biomass inputs, expressed as CO_2 equivalent (CO_2-eq), kg/hm^2. No exogenous organic matter was added in this study, so it was 0;

GWP_{output}—Warming potential for economic production and biomass output, expressed as CO_2 equivalent (CO_2-eq), kg/hm^2;

GWP_{GHGs}—Warming potential of soil heterotrophic respiration, soil emissions of N_2O and total CH_4 emissions, expressed as CO_2 equivalent (CO_2-eq), kg/hm^2. The combined greenhouse effect caused by each kilogram of CH_4 and N_2O on a 100-year scale is 25 and 298 times that of CO_2, respectively.

$GWP_{indiret}$—Warming potential from various farm material inputs, expressed as CO_2 equivalent (CO_2-eq), kg/hm^2. The relevant parameters are shown in Table 4.

When *NGWP* > 0, greenhouse agroecosystems behave as sinks of greenhouse gases and vice versa.

Table 4. Greenhouse gas emission factors for different material inputs.

Item	GHG Coefficients (CO_2-ep)	Farm Inputs of Different Treatments				
		Unit	N$_1$C	N$_1$A	N$_2$C	N$_2$A
N	4.80 (kg·kg^{-1})	kg·hm^{-2}	120	120	180	180
P_2O_5	1.14 (kg·kg^{-1})	kg·hm^{-2}	120	120	180	180
K_2O	0.60 (kg·kg^{-1})	kg·hm^{-2}	136.8	136.8	234	234
Agrochemical	6.58 (kg·kg^{-1})	kg·hm^{-2}	3	3	3	3
Electrical power	0.92 (kg/kW·h)	kW·h	200	280	200	280
Mulch	5.18 (kg·kg^{-1})	kg·hm^{-2}	60	60	60	60
Tillage	15.2 (kg/hm^2)	hm^{-2}	3	3	3	3
Spray	1.4 (kg/hm^2)	Order	4	4	4	4
Ridges on ridges	0.25 (kg/P·d)	P.·d	4	4	4	4
Film covering	0.25 (kg/P·d)	P.·d	4	4	4	4
Harvest	22.9 (kg/hm^2)	Order	3	3	3	3
Fertilize	0.4 (kg/hm^2)	Order	5	5	5	5

(2)   Soil and crop-based approach, S&CBA

$$NGWP = GWP_{NPP} + GWP_{\triangle SOC} - GWP_{GHG_s} - GWP_{indiret} \tag{6}$$

NGWP—Integrated greenhouse effect, expressed as CO_2 equivalent (CO_2-eq), kg/hm^2;

GWP_{NPP}—Warming potential of net primary productivity, expressed as CO_2 equivalent (CO_2-eq), kg/hm^2;

$GWP_{\triangle SOC}$—The warming potential of the change in organic carbon content before and after the experiment was set to 0 because the experiment was negligible for only one season.

GWP_{GHGs}—Warming potential of total soil CO_2 (biomass is partially reintroduced into the field and released into the atmosphere as carbon dioxide [22]), N_2O, and CH_4 emissions, kg/hm^2, in CO_2 equivalent, where the combined greenhouse effect (*GWP*) caused by each kg of CH_4 and N_2O on a 100-year scale is 25 and 298 times higher than that of CO_2, respectively.

When *NGWP* > 0, the greenhouse farmland ecosystem is a greenhouse gas sink. When *NGWP* < 0, it is a greenhouse gas source.

2.5.5. Water Use Efficiency

Water use efficiency (WUE) It is the mass of dry matter ($kg \cdot m^{-3}$) that can be accumulated per unit volume of water consumed by a crop ecosystem.

Partial fertilizer productivity (PFP) is the crop fruit yield (kg/kg) that can be produced per unit of fertilizer input [23].

2.6. Data Processing and Analysis

Microsoft Excel 2016 (Microsoft Corp., 2016, Redmond, WA, USA) software was used for data processing and plotting; SPSS Statistics 25 (IBM Corp., 2017, Armonk, NY, USA) was used to analyze the experimental data; Origin2022 (OriginLab Corp., 2022, Northampton, MA, USA) was used for plotting; and the crop-based approach (CBA) and soil and crop-based approach (S&CBA) were applied to calculate and evaluate the carbon sequestration capacity of greenhouse agroecosystems.

3. Results and Analysis

3.1. Yield and GHG Emissions

3.1.1. Yield and Biomass

Figure 2 presents the yield and biomass of greenhouse tomato under different treatments. Yield and biomass were generally higher under nano-bubble irrigation than under conventional irrigation. Nano-bubble irrigation increased the yield by 18.94% and 16.36% ($p < 0.05$) and biomass by 10.78% and 17.98% ($p < 0.05$) under low and normal nitrogen conditions, respectively, compared with conventional irrigation. Nano-bubble irrigation significantly increased the yield and biomass of greenhouse tomato, resulted in a high crop yield, and helped achieve carbon sequestration and emission reduction.
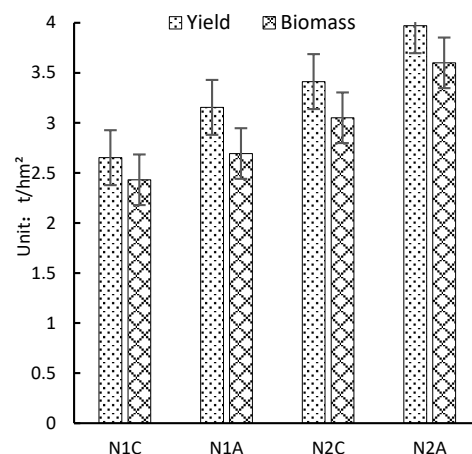

Figure 2. Yield and biomass of different treatments.

3.1.2. Dynamics of N_2O, CO_2 and CH_4 Emissions

The GHG emissions fluxes were calculated to obtain total GHG emissions. The greenhouse tomato soil was the "source" of CO_2 and N_2O emissions and the absorption "sink" of CH_4 (T.5), in which the degree of influence of each GHG on the greenhouse effect was as follows: $CO_2 > N_2O > CH_4$. CO_2 and N_2O are the main components of the net global warming potential (NGWP), while the contribution of CH_4 is negligible.

Figure 3 lists the soil N_2O emission dynamics of the greenhouse tomato plots under different treatments. During the complete life span of tomato, N_2O emission fluxes exhibited obvious temporal variability. Each treatment displayed an overall upward trend, with short emission peaks at the end of the flowering and fruit-bearing periods (56 days after transplanting), at the beginning of fruit expansion (72 days after transplanting), and in the rest of the period. During the rest of the period, these N_2O emission fluxes were relatively low and exhibited small fluctuations. During the complete life span of tomato, the maximum value of N_2O emission flux was 570.89 $\mu g \cdot m^{-2} \cdot h^{-1}$ (72 days after transplanting in N_2A treatment). Compared with the conventional irrigation, the main peak of the flux increased by 47.31% and 34.76% under the low and normal nitrogen conditions, respectively, with nano-bubble irrigation ($p < 0.05$). Moreover, a highly significant N_2O emission flux subpeak of 569.06 $\mu g \cdot m^{-2} \cdot h^{-1}$ was noted during the flowering and fruit-bearing periods (56 days after transplanting in N_2A treatment), which was 76.11%, 52.93%, and 37.89% higher than that after transplanting in N_1C, N_1A, and N_2C treatments, respectively ($p < 0.05$).
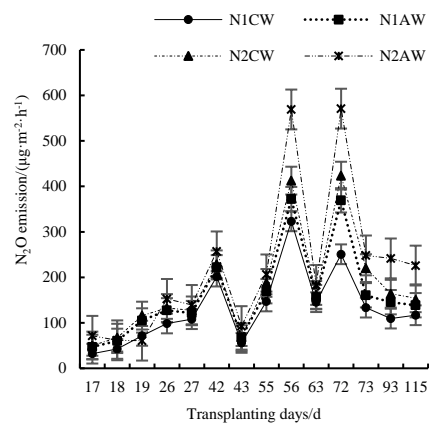

Figure 3. N_2O flux in different treatments.

Figure 4 presents the soil CO_2 emission dynamics in greenhouse tomato plots under different treatments. The CO_2 emission fluxes of tomato treatments changed consistently throughout the whole tomato lifecycle, exhibiting obvious time-varying characteristics and an increasing trend over time. The CO_2 emission fluxes continued to increase to the peak from the flowering and fruit-bearing period (42 days after transplanting) and then declined. However, the fluxes continued to be extremely high until the end of the reproductive period. The CO_2 emission flux at the beginning of fruit expansion (6 days after transplanting) had a peak value of 546.37 $mg \cdot m^{-2} \cdot h^{-1}$ (63 days after transplanting in the N_2A treatment). The main peak values of the fluxes of low and normal nitrogen inputs increased by 5.71% and 13.44%, respectively, compared with that of the water–fertilizer–gas integration. Starting from the flowering and fruit-bearing periods (42 days after transplanting), the CO_2 emission flux of the nano-bubble irrigation treatment was significantly higher than that of the conventional irrigation treatment, and then gradually converged to the level similar to that at the beginning of fruit expansion (72 days after transplanting).
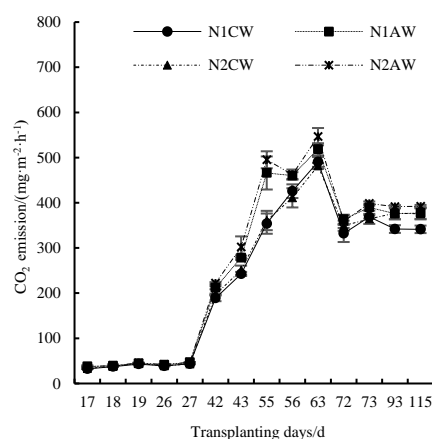
Figure 4. CO_2 flux in different treatments.

Figure 5 presents the soil CH_4 emission dynamics of greenhouse tomato plots under different treatments. The soil CH_4 emission fluxes of each treatment basically exhibited negative emissions during the entire tomato lifecycle, that is, the soil served as a sink for CH_4. During the study period, CH_4 emission fluxes exhibited a trough value of -137.36 $\mu g \cdot m^{-2} \cdot h^{-1}$ at the beginning of flowering and fruiting (19 days after transplanting in the N_2A treatment). The main peaks of negative soil CH_4 emission fluxes increased by 207.39% and 26.90% during nano-bubble irrigation under the low and normal nitrogen conditions, respectively. Moreover, CH_4 emission fluxes displayed a positive emission peak of 37.42 $\mu g \cdot m^{-2} \cdot h^{-1}$ during the late harvesting period (72 days after transplanting in the N_1C treatment).

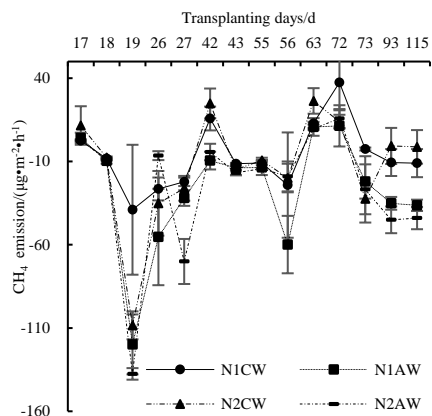**Figure 5.** CH_4 efflux in different treatments.

3.2. Net Greenhouse Warming Potential (NGWP) of Farmland

The net greenhouse warming potential (NGWP) of each treatment was obtained using two calculation and evaluation systems: crop-based approach (CBA) method and soil and crop-based approach (S&CBA) method (Table 5). The carbon sequestration unit of the CBA method is the biomass of the greenhouse farmland, and its value is considerably greater than the direct and indirect emissions of GHG. This indicates that greenhouse farm ecosystems are a sink for GHGs, and the main source is related to the biomass carbon sequestration capacity of crops. The carbon sequestration capacity of crops under different treatments was in the order of $N_2A > N_2C > N_1A > N_1C$. Under nano-bubble irrigation, the NGWP values for the low and normal nitrogen treatments increased by 6.93% and 53.28%, respectively ($p < 0.05$). The S&CBA method considered NPP and ΔSOC, which mainly depend on the crop yield. The higher the crop yield, the more the fixed carbon and the higher the carbon sequestration potential of crops. The magnitude of carbon sequestration capacity of crops under different treatments was in the order of

$N_2A > N_2C > N_1A > N_1C$, and NGWP values increased by 22.69% and 14.52% under low and normal nitrogen conditions, respectively, during nano-bubble irrigation compared with during conventional irrigation ($p < 0.05$).

Table 5. Net greenhouse warming potential under different treatments, in kg·hm^{-2}.

| Method | Treatment | GWP$_{NPP}$ | | GWP$_{GHGs}$ | | | GWP$_{indiret}$ | NGWP |
		Yield	Biomass	CO$_2$	N$_2$O	CH$_4$		
Crop-based approach, CBA	N$_1$C	–	10,213.21 ± 144.59	6583.23 ± 14.48	800.07 ± 10.28	−4.32 ± 1.67	1433.32	1400.92 ± 160.43
	N$_1$A	–	11,314.56 ± 179.7	7288.72 ± 87.54	1038.20 ± 12.35	−17.32 ± 1.78	1506.92	1498.04 ± 162.93
	N$_2$C	–	12,815.70 ± 261.82	7252.01 ± 54.86	1088.97 ± 9.14	−6.39 ± 2.38	1779.64	2701.47 ± 206.03
	N$_2$A	–	15,119.69 ± 255.52	7665.86 ± 30.75	1478.18 ± 10.6	−18.48 ± 0.28	1853.24	4140.88 ± 237.36
Soil&crop-based approach, S&CBA	N$_1$C	26,526.03 ± 242.44	–	6583.23 ± 14.48	800.07 ± 10.28	−4.32 ± 1.67	1433.32	17,713.74 ± 219.52
	N$_1$A	31,549.60 ± 335.04	–	7288.72 ± 87.54	1038.20 ± 12.35	−17.32 ± 1.78	1506.92	21,733.09 ± 413.17
	N$_2$C	34,126.33 ± 187.35	–	7252.01 ± 54.86	1088.97 ± 9.14	−6.39 ± 2.38	1779.64	23,090.27 ± 429.09
	N$_2$A	39,709.42 ± 408.06	–	7665.86 ± 30.75	1478.18 ± 10.6	−18.48 ± 0.28	1853.24	26,442.97 ± 470.08

The results obtained using different research methods in the same discussion object are highly inconsistent. This difference is mainly a result of the difference in the carbon sequestration carriers, that is, different categories of carbon sequestration units. However, both the aforementioned methods exhibited that nano-bubble irrigation can significantly improve the carbon sequestration capacity of crops. The S&CBA evaluation method considers both GHGs and crop yields in greenhouse farmland, which is more appropriate for China, as it has a large population and needs to maintain food security [24].

Figure 6 presents the greenhouse effect produced by soil GHGs during the complete reproductive period of greenhouse tomato under different treatments. The greenhouse effect produced by CO$_2$ was considerably higher than that produced by the remaining two gases (N$_2$O and CH$_4$). The greenhouse effect produced by CH$_4$ was minimal and negligible. Because of the negative correlation between the greenhouse effect caused by soil GHG emissions and NGWP, CO$_2$ exerted the strongest effect on NGWP and significantly reduced it. CH$_4$ had the least, but a positive, effect on NGWP. The greenhouse effect produced under nano-bubble irrigation treatments was higher than that produced under conventional irrigation, regardless of whether the input was low or normal nitrogen. CO$_2$ increased by 10.72% and 5.71% ($p < 0.05$), and N$_2$O increased by 29.76% and 35.74% ($p < 0.05$) under low and normal nitrogen conditions, respectively.
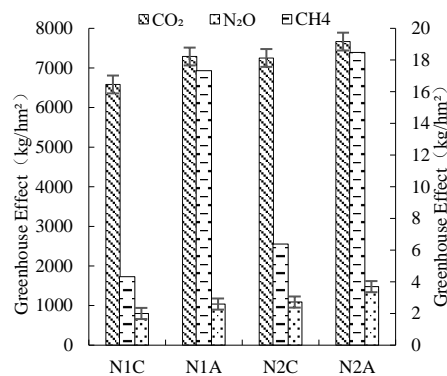

Figure 6. Greenhouse effect caused by different treatments of greenhouse gases.

3.3. The Relationship between Yield, Water and Nitrogen Utilization Efficiency, and Warming Potential

Table 6 presents the significant relationships between tomato yield, water and nitrogen use efficiencies, nitrogen fertilizer partial productivity, and the overall greenhouse effect under different fertilization conditions and in the presence of dissolved oxygen levels. Compared with conventional irrigation, nano-bubble irrigation has substantial advantages. Nano-bubble technology significantly increased the crop yield and improved water and fertilizer utilization efficiencies. Specifically, with nano-bubble irrigation, the yield of crops subjected to low and normal nitrogen treatments increased by 18.94% and 16.36%, respectively ($p < 0.05$). Similarly, the nutrient use efficiency (NUE) and partial fertilizer productivity (PFP) increased by 7.28% and 1.53% ($p < 0.05$) and 19.39% and 17.05%, respectively ($p < 0.05$). Additionally, the overall greenhouse effect under the two treatments increased by 22.69% and 14.52%, respectively ($p < 0.05$).

Table 6. The relationship between crop yield, nitrogen utilization efficiency, partial fertilizer productivity, and net greenhouse warming potential under different treatments.

Treatment	Yield	NUE	PFP	NGWP
N_1C	26,526.03 ± 242.44 d	345.79 ± 24.28 b	221.05 ± 2.02 b	17,713.74 ± 219.52 d
N_1A	31,549.60 ± 335.04 c	370.98 ± 10.83 b	263.91 ± 1.33 a	21,733.09 ± 413.17 c
N_2C	34,126.33 ± 187.35 b	414.89 ± 18.09 a	189.22 ± 0.49 c	23,090.27 ± 429.09 b
N_2A	39,709.42 ± 408.06 a	421.24 ± 12.95 a	221.48 ± 0.76 b	26,442.97 ± 470.08 a
F				
N	199.96 **	35.57 **	248.15 **	48.91 **
A	90.57 **	2.48	253.84 **	36.13 **
N×A	2.52	0.89	50.54 *	2.137

Note: Different lowercase letters in the same column indicate significant differences ($p < 0.05$), * means $p < 0.05$, ** means $p < 0.01$.

The nitrogen application rate and air addition rate significantly affected the yield, PFP, and NGWP ($p < 0.01$) under a single factor. The nitrogen application rate also significantly influenced the NUE ($p < 0.05$). Additionally, the interaction between the nitrogen application rate and the nano-bubble irrigation rate significantly affected PFP ($p < 0.05$).

3.4. Soil Environmental Factors and GHGs

3.4.1. Soil Environmental Factors

The soil temperature of different treatments varied slightly (Figure 7a), with the temperature fluctuating within the temperature range of 15–32 °C during the whole reproductive period in the test, similarly to the dynamic change in the air temperature of the greenhouse. The trend of water content in 20 cm water-filled pore space (WFPS) of each treatment was consistent. Irrigation was the primary cause of elevated soil WFPS, and fertilization had no significant effect on WFPS. On comparing the mean WFPS values of four irrigation cycles under different dissolved oxygen levels, we observed that under nano-bubble irrigation, the WFPS of soil receiving low and normal nitrogen inputs decreased by 2.85% and 5.17%, respectively (Figure 7a). The temporal dynamics of soil ODR, DO, and E_h during four consecutive irrigation cycles are presented in Figure 7b, Figure 7c, and Figure 7d, respectively. The trends of ODR, DO, and E_h changes in different treatments were the same. The ODR, DO, and E_h values decreased rapidly after the irrigation treatments, and then gradually increased and stabilized. Under the experimental conditions, different levels of nitrogen applied exerted no significant effect on soil ODR, DO, and E_h. However, after nano-bubble irrigation, the ODR, DO, and E_h values increased by 9.16% and 10.14%, 8.71% and 8.82%, and 4.43% and 10.94%, respectively, under low versus normal nitrogen conditions ($p < 0.05$).
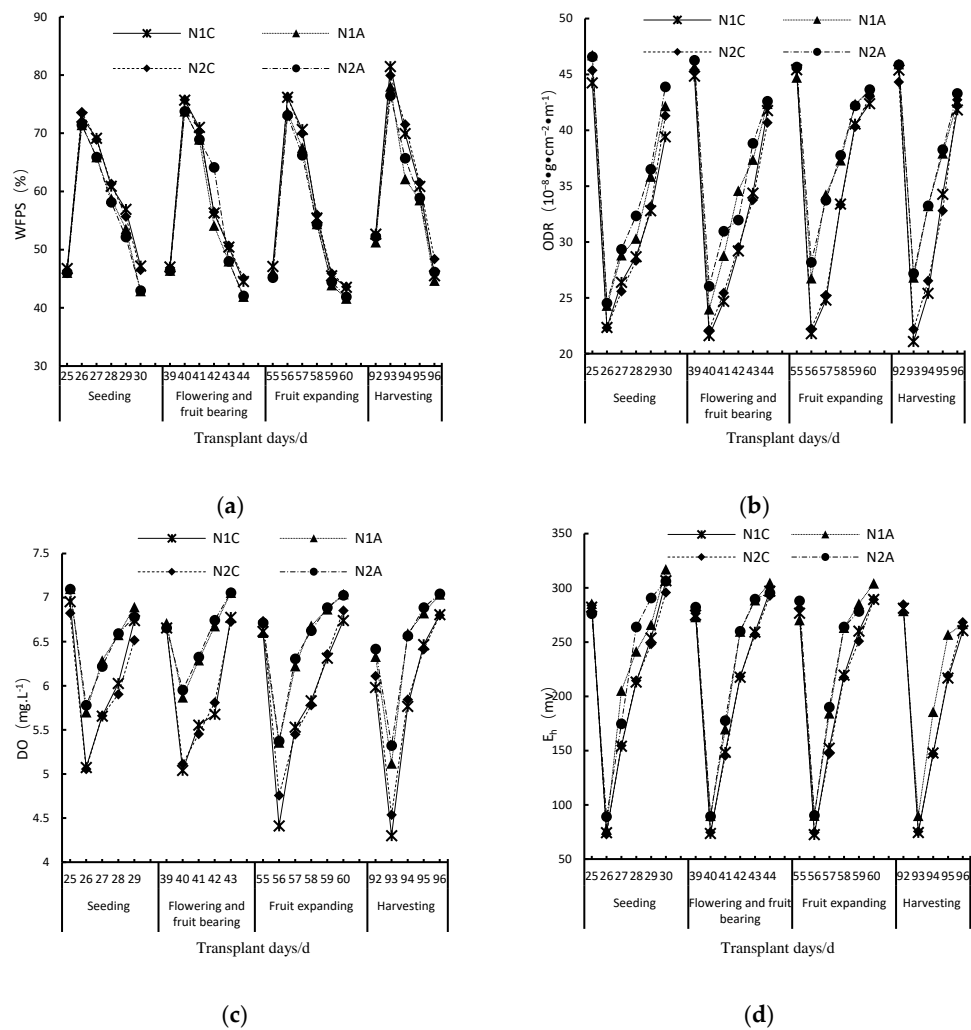
(**a**)

(**b**)

(**c**)

(**d**)

Figure 7. Each processing 0–20 cm soil environmental factors change trend. (**a**) 0–20 cm WFPS. (**b**) 0–20 cm ODR. (**c**) 0–20 cm DO. (**d**) 0–20 cm E_h.

3.4.2. Correlation between Soil Environmental Factors and GHGs

The experimental data were analyzed using SPSS 22.0 to determine the coefficients of correlation between GHG emissions and soil physicochemical factors after the application of nano-bubble irrigation (Figure 8). ODR, DO, and E_h of soil exhibited significant positive correlations ($p < 0.01$) with N_2O emissions, but a significant negative correlation ($p < 0.01$) with CH_4 emissions. On the other hand, WFPS exhibited a significant positive correlation ($p < 0.01$) with CH_4 emissions, but a significant negative correlation ($p < 0.01$) with N_2O emissions. ODR, DO, and E_h were positively correlated with CO_2.
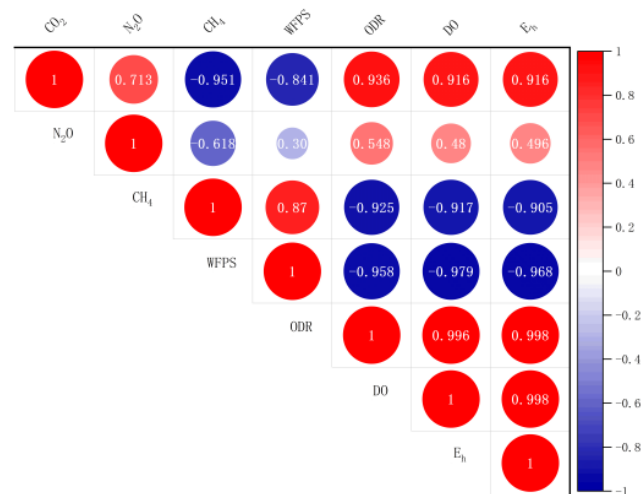
Figure 8. Correlation between greenhouse gas emissions and environmental factors.

4. Discussion

4.1. Causes of Dynamic Changes in GHGs at Different Growth Stages

4.1.1. Causes of Changes in N_2O Emissions

Irrigation, fertilization, and temperature influence the emission of N_2O, a byproduct of nitrification and denitrification processes of soil microorganisms. Of these factors, temperature exerts its effects by influencing soil microbe activity. Numerous studies have reported an exponential positive correlation between N_2O emissions and temperature [25]. Denitrification increases within 10–30 °C [26]. The N_2O emission flux here exhibited an overall increasing trend during the entire tomato growth period, possibly because of the gradually increasing soil temperature, which promotes N_2O emissions. Such fluctuations in the emission flux may also be attributable to changes in the irrigation volume with an increase in the number of transplanting days. Soil microbes cause denitrification after irrigation, thereby resulting in these fluctuations [27]. Consequently, under the combined influences of temperature and irrigation, the N_2O emission flux thus presents an overall increasing trend with intermittent fluctuations. N_2O emission flux is positively correlated with WFPS when it is lower than a certain threshold. When WFPS reaches 70%, N_2O emission flux is the largest [28,29]. The present study confirmed this observation; two short emission peaks were observed during the end of the flowering and fruit-bearing period (56 days after transplanting) and the fruit expansion period (72 days after transplanting), when the WFPS was approximately 70%. Additionally, N_2O emissions under the normal nitrogen condition were higher than those under the low nitrogen condition in this study. This discrepancy is attributable to direct provision of sufficient nitrogen to N_2O producers by nitrogen fertilizers, which then affects the soil NO_3-N content and consequently increases soil N_2O emissions [30].

4.1.2. Causes of Changes in CO_2 Emissions

CO_2 emissions occur due to the microbial decomposition of carbon-containing organic matter. In particular, they are mainly caused by the decomposition of soil organic matter, and the respiration of soil microbes, soil animals, and plant root and rhizosphere microorganisms [31]. During this study, the CO_2 emission flux from the soil was 30 to 600 mg/($m^2 \cdot h^1$), which was significantly higher than that observed in field experiments [32,33]. The soil CO_2 emission flux during the entire tomato growth period exhibited visible time-varying characteristics and generally increased over time. This increase may have been a result of the gradually increasing soil temperature during the growth period, as studies have reported a strong correlation among temperature, humidity, and CO_2 emissions [34]. However, the emission flux was relatively low during the seedling stage, possibly because two irrigations during this stage significantly increased the soil water

content, thereby creating an anaerobic environment, which then inhibited the microbial activity and consequently reduced soil respiration. Additionally, irrigation can inhibit or promote CO_2 emissions by influencing plant root respiration and altering soil permeability. Dry soils tend to emit higher CO_2 content compared with wet soils [35]. The peak in CO_2 emissions was noted during the middle and late flowering and fruit-bearing stages of tomato plants as well as during the early fruit expansion period. During these stages, nutrients were concentrated to support plant growth, with the root quality continuing to improve and the number of microorganisms gradually increasing throughout the growth period. All of these factors contributed to the CO_2 emissions reaching the peak level [36,37].

4.1.3. Causes of Changes in CH_4 Emissions

CH_4 is formed in soil by the combined action of anaerobic bacteria (methanogens) and aerobic bacteria [38]. When oxygen is absent, methanogens break down soil organic matter, resulting in CH_4 production and its subsequent emission. In an oxygen-rich environment, aerobic bacteria oxidize CH_4 into CO_2 [39]. Figure 7c illustrates the soil CH_4 emission flux throughout the tomato growth period, which generally exhibited a negative emission state. However, CH_4 emissions could still occur during specific periods, such as 1–2 days after irrigation. This may be attributable to excessive moisture in the local soil due to a mulching film-induced sudden influx of water [40]. Rapid organic matter decomposition stimulates the activity of methanogens, causing a temporary increase in the CH_4 emission flux. Under the same irrigation regime, nitrogen application can increase the CH_4 emission flux from soil respiration, possibly because higher nitrogen input increases the abundance of methanogenic bacteria, thus resulting in an increase in CH_4 emissions [41]. Furthermore, under the same fertilization pattern, soil methane emissions decrease with an increase in the dissolved oxygen levels. This is because injecting oxygen-rich water into the crop root soil increases the number and activity of methanogens. Consequently, the growth rate of methanogens slows down, leading to a negative emission state for the soil CH_4 flux.

4.2. Effects of Nano-Bubble Irrigation on the Yield and GHG Emissions

Nano-bubble irrigation can significantly improve the soil microenvironment. This improvement is beneficial for crop root growth, which then increases the crop yield and biomass and affects soil GHG (N_2O, CH_4, CO_2) emissions [42,43].

In this study, nano-bubble irrigation significantly improved tomato yield compared with conventional irrigation under the same fertilization conditions. Specifically, compared with conventional irrigation, the yield increased by 18.94% and 16.36% ($p < 0.05$) under low and normal nitrogen treatments, respectively. The increase in yield was higher under the low nitrogen condition, suggesting that this treatment had a better yield-enhancing effect during nano-bubble irrigation. The study findings differ from those of a study by Lei et al., in which normal nitrogen treatment was reported as the most suitable fertilizer input for tomato growth in the nano-bubble combination scheme. This difference in results could potentially be caused by the interaction of other factors influencing the optimal outcomes of nano-bubble irrigation [44].

We here evaluated the NGWP of greenhouse farmland under different treatments. The results showed that the greenhouse farmland ecosystem serves as a greenhouse gas sink. Nano-bubble irrigation exhibited better carbon sequestration and emission reduction effects, particularly under the low nitrogen condition. Compared with conventional irrigation, NGWP increased by 22.69% and 14.52% under the low and normal nitrogen treatments, respectively ($p < 0.05$). These findings suggest that nano-bubble irrigation can improve carbon sequestration and reduce emissions, especially when combined with a low nitrogen input. Nitrification is further promoted by the increase in fertilizer application, improved soil hydrothermal conditions, and appropriate implementation of mulching measures for nitrogen accumulation. Nano-bubble irrigation technology improves soil permeability in the root zone, offering favorable conditions for NO_2 emissions. The greenhouse facility provides good control over hydrothermal conditions. Moreover, nano-bubble irrigation

delivers oxygen-rich water to the crop root zone, triggering changes in soil aeration, soil microorganisms, and the physical and chemical microenvironment of the rhizosphere [45,46]. These changes inevitably affect the GHG emissions flux of soil and contribute positively to the carbon sequestration and emission reduction of greenhouse tomatoes.

4.3. Improvement Measures

4.3.1. Exogenous Organic Matter Is Applied to Promote Carbon Sequestration and Emission Reduction

The addition of biochar to soil is known to have several benefits. First, biochar reduces deposit density [47]. The soil physical quality can also be improved by adjusting the pyrolysis conditions and using biochar prepared from different types of biomass [48]. Additionally, the high pore structure of biochar aids in soil water retention [49]. Furthermore, biochar applied to soil is known to significantly reduce N_2O emissions [50]. Nano-bubble irrigation technology can enhance soil aeration, increase yield, sequester carbon, and promote soil health. Organic fertilizers can improve soil physical and chemical properties, and the integration of organic amendments can enhance soil microbial diversity [51]. These practices can improve soil permeability and water retention, and stimulate crop growth and root metabolism. They can also effectively reduce GHG emissions [52,53] and accelerate the rate of soil microbe propagation [54]. When nano-bubble irrigation technology is implemented, the use of organic fertilizers and nitrification inhibitors must be appropriately managed [55]. This approach can effectively reduce N_2O emissions from agricultural soil.

4.3.2. The Applicability of Nano-Bubble Irrigation Can Be Strengthened through Extensive Popularization

Ensuring food security is a global challenge [56]. In China's agricultural development, the low water and fertilizer utilization rates pose a major problem. One solution to improve crop yield, carbon sequestration, and emissions reduction is to adopt nano-bubble drip irrigation technology, which has gained widespread attention in agricultural production. This technology promotes sustainable agricultural development [57]. First, for the wide adoption of nano-bubble systems, the technology should offer advantages such as automation, easy operation, and targeted application. Additionally, the cost of implementing this technology should be manageable and not adversely affect economic benefits while achieving agricultural modernization. Second, the nano-bubble irrigation systems should be responsive to soil aeration conditions. Soil aeration must be improved for enhancing soil eco-physical conditions and increasing crop yield and productivity [58]. Considering the variations in crop growth conditions across different natural environments, nano-bubble irrigation technology must be continuously refined and tested. Optimizing the technical parameters of related instruments for different field environments is crucial, as it would improve the practicality and applicability of nano-bubble irrigation technology.

5. Conclusions

(1) Nano-bubble irrigation has been shown to improve water use efficiency and nutrient uptake in crops, resulting in a significant increase in crop yield. Compared to conventional methods, nano-bubble irrigation led to an 18.94% and 16.36% increase in yield ($p < 0.05$) under low and normal nitrogen conditions, respectively. Additionally, this new technology enhanced nitrogen use efficiency (NUE) by 7.28% and 1.53% ($p < 0.05$) and increased partial fertilizer productivity (PFP) by 19.39% and 17.05% ($p < 0.05$), respectively, under the same conditions.

(2) The influence of a single factor, such as nitrogen application rate or air addition, had an extremely significant effect on yield ($p < 0.01$). However, the interaction between the nitrogen application rate and nano-bubble irrigation did not have a significant effect on yield but showed a significant effect on PFP ($p < 0.05$) under multiple factor interactions.

(3) In greenhouses, tomato soil under nano-bubble irrigation acts as both a source of CO_2 and N_2O emissions and an absorption sink of CH_4. The greenhouse effect was found

to be influenced in the order of $CO_2 > N_2O > CH_4$, with the greenhouse farmland ecosystem serving as a sink for greenhouse gases. Compared to conventional irrigation, nano-bubble irrigation increased the net global greenhouse potential (NGWP) values under low and normal nitrogen conditions by 22.69% and 14.52%, respectively ($p < 0.05$).

(4) By combining nano-bubble irrigation with organic amendments, it is possible to achieve increased crop yield, carbon sequestration, and emissions reduction, thus improving the practicality and applicability of this novel irrigation technology.

In conclusion, nano-bubble irrigation has a positive impact on crop yield, water and fertilizer utilization efficiencies, and carbon sequestration in the greenhouse farmland ecosystem.

References

1. UNEP. *The Global Launch of the Emissions Gap Report*; United Nation Environment Programme: Nairobi, Kenya, 2013.
2. Oldfield, E.E.; Eagle, A.J.; Rubin, R.L.; Rudek, J.; Sanderman, J.; Gordon, D.R. Crediting agricultural soil carbon sequestration. *Science* **2022**, *375*, 1222–1225. [CrossRef] [PubMed]
3. Wang, L.J.; Bai, Y.; Wang, J.Y.; Qin, F.; Li, C.; Zhou, Z.; Jiao, X.H. A Transferable Learning Classification Model and Carbon Sequestration Estimation of Crops in Farmland Ecosystem. *Remote Sens.* **2022**, *14*, 5216. [CrossRef]
4. Souza, C.F.; Sala, F.C.; Faez, R. Polymer fertilizer and the fertigation of grape tomatoes in protected cultivation. *Sci. Hortic.* **2023**, *311*, 111801. [CrossRef]
5. Yu, X.M.; Zhang, J.W.; Yuhui Zhang, Y.H. Identification of optimal irrigation and fertilizer rates to balance yield, water and fertilizer productivity, and fruit quality in greenhouse tomatoes using TOPSIS. *Sci. Hortic.* **2023**, *311*, 111829. [CrossRef]
6. Velasco, N.F.; Ligarreto, G.A.; Díaz, H.R.; Fonseca, L.P.M. Photosynthetic responses and tolerance to root-zone hypoxia stress of five bean cultivars (*Phaseolus vulgaris* L.). *S. Afr. J. Bot.* **2019**, *123*, 200–207. [CrossRef]
7. Habibi, F.; Liu, T.; Shahid, M.A.; Schaffer, B.; Sarkhosh, A. Physiological, biochemical, and molecular responses of fruit trees to root zone hypoxia. *Environ. Exp. Bot.* **2023**, *206*, 105179. [CrossRef]
8. Lei, H.J.; Jin, C.C.; Hu, S.G.; Pan, H.W.; Li, Y.P.; Wang, L.Y. Effect of aerated subsurface drip irrigation on soil ventilation of Solanum purpurei in greenhouse. *J. Jiangsu Univ. Nat. Sci. Ed.* **2019**, *40*, 325–331. (In Chinese)
9. Zhou, H.L.; Xu, P.J.; Zhang, L.J. Effects of regulated deficit irrigation combined with optimized nitrogen fertilizer management on resource use efficiency and yield of sugar beet in arid regions. *J. Clean. Prod.* **2022**, *380*, 134874. [CrossRef]
10. Qian, H.; Zhu, X.; Huang, S.; Linquist, B.; Kuzyakov, Y.; Wassmann, R.; Minamikawa, K.; Martinez-Eixarch, M.; Yan, X.; Zhou, F.; et al. Greenhouse gas emissions and mitigation in rice agriculture. *Nat. Rev. Earth Environ.* **2023**, *4*, 716–732. [CrossRef]
11. Jin, C.C.; Liu, H.J.; Chen, J.; Xiao, Z.Y.; Leghari, S.J.; Yuan, T.; Pan, H.W. Effect of Soil Aeration and Root Morphology on Yield under Aerated Irrigation. *Agronomy* **2023**, *13*, 369. [CrossRef]
12. Chen, H.; Liu, W.; Shang, Z.H.; Zhu, Y.; Cai, H.J. Response of deficit irrigation on soil CO_2 and N_2O emissions in greenhouse tomato fields. In Proceedings of the 2021 ASABE Annual International Meeting, Virtual Meeting, 12–16 July 2021.
13. Tack, J.; Barkley, A.; Hendricks, N. Irrigation offsets wheat yield reductions from warming temperatures. *Environ. Res. Lett.* **2017**, *12*, 114027. [CrossRef]
14. Maneepitak, S.; Ullah, H.; Datta, A.; Shrestha, R.P.; Shrestha, S.; Kachenchart, B. Effects of water and rice straw management practices on water savings and greenhouse gas emissions from a double-rice paddy field in the Central Plain of Thailand. *Eur. J. Agron.* **2019**, *107*, 18–29. [CrossRef]

15. Baram, S.; Weinstein, M.; Evans, J.F.; Berezkin, A.; Sade, Y.; Ben-Hur, M.; Bernstein, N.; Mamane, H. Drip irrigation with nanobubble oxygenated treated wastewater improves soil aeration. *Sci. Horticult.* **2022**, *291*, 110550. [CrossRef]

16. Bo, Y.; Jägermeyr, J.; Yin, Z.; Jiang, Y.; Xu, J.Z.; Liang, H.; Zhou, F. Global benefits of non-continuous flooding to reduce greenhouse gases and irrigation water use without rice yield penalty. *Glob. Change Biol.* **2022**, *28*, 3636–3650. [CrossRef] [PubMed]

17. Lei, H.J.; Yang, H.G.; Liu, H.; Pan, H.W.; Liu, X.; Zang, M. Characteristics and influencing factors of N_2O emission in tomato soil under nano-bubble coupled drip irrigation. *J. Jiangsu Univ. Nat. Sci. Ed.* **2019**, *35*, 95–104. (In Chinese)

18. Singh, J.; Singh, B.; Sharma, S. Comparison of soil carbon and nitrogen pools among poplar and eucalyptus based agroforestry systems in Punjab, India. *Carbon Manag.* **2021**, *6*, 12. [CrossRef]

19. Li, Y.; Liu, S.; Yang, X.; Wu, C.; Gao, Q.; Zhang, L. The Influence of Applying Microbial Amendments to Soil and Plants on the Microbial Diversity in the Rhizosphere Soil of Garlic. *J. Biobased Mater. Bioenergy* **2021**, *4*, 15. [CrossRef]

20. Han, Y.; Lu, H.; Qiao, D. Integrated effects of meteorological factors, edaphic moisture, evapotranspiration, and leaf area index on the net primary productivity of Winter wheat—Summer maize rotation system. *Field Crop. Res.* **2023**, *302*, 109080. [CrossRef]

21. Hang, H.Y.; Kim, G.W.; Kim, S.Y.; Mozammel Haque, M.; Khan, M.I.; Kim, P.J. Effect of cover cropping on the net global warming potential of rice paddy soil. *Geoderma* **2017**, *292*, 49–58.

22. Deshmukh, C.S.; Susanto, A.P.; Nardi, N.; Nurholis, N.; Kurnianto, S.; Suardiwerianto, Y.; Hendrizal, M.; Rhinaldy, A.; Mahfiz, R.E.; Desai, A.R.; et al. Net greenhouse gas balance of fibre wood plantation on peat in Indonesia. *Nature* **2023**, *616*, 740–746. [CrossRef]

23. Li, Y.P.; Zhang, F.C.; Hou, X.H.; Yan, F.L.; Xiao, C.; Li, J.; Cheng, H.L. Effects of planting density and interaction of water and nitrogen on cotton growth and water and nitrogen utilization in southern Xinjiang. *JNWAFU* **2021**, *49*, 45–56+66. (In Chinese)

24. Liu, X.H.; Xu, W.W.; Li, Z.J.; Chu, Q.Q.; Yang, X.L.; Chen, B. Carbon footprint method of farmland ecosystem: Misunderstanding, improvement and application: An analysis of carbon efficiency of intensive farming in China. *China J. Agric. Res. Reg. Plan.* **2014**, *35*, 1–7. (In Chinese)

25. Chen, H.; Hou, H.; Hu, H.; Shang, Z.; Zhu, Y.; Cai, H.; Qaisar, S. Aeration of different irrigation levels affects net global warming potential and carbon footprint for greenhouse tomato systems. *Sci. Hortic.* **2018**, *242*, 10–19. [CrossRef]

26. Cui, P.Y.; Fan, F.L.; Yin, C. Long-term organic and inorganic fertilization alters temperature sensitivity of potential N_2O emissions and associated microbes. *Soil Biol. Biochem.* **2016**, *93*, 131–141. [CrossRef]

27. Matson, P.A.; Naylor, R.; Ortiz-Monasterio, I. Integration of environmental, agronomic, and economic aspects of fertilizer management. *Science* **1998**, *280*, 112–115. [CrossRef]

28. Li, F.Y.; Yuan, C.Y.; Lao, D.Q.; Yao, B.L.; Hu, X.F.; You, Y.J.; Wang, L.; Sun, S.B.; Liang, X.Q. Drip irrigation with organic fertilizer application improved soil quality and fruit yield. *Agron. J.* **2020**, *112*, 608–623. [CrossRef]

29. Wang, X.; Jlang, Y.L.; Jla, B.R.; Wang, F.; Zhou, G.S. Comparison of soll respiratlon among three temperate forests in Changbal Mountains, China. *Can. J. For. Res.* **2010**, *40*, 788–795. [CrossRef]

30. Zhou, S.; Sun, H.; Bi, J.; Zhang, J.; Riya, S.; Hosomi, M. Effect of water-saving irrigation on the N_2O dynamics and the contribution of exogenous and endogenous nitrogen to N2O production in paddy soil using 15N tracing. *Soil Tillage Res.* **2020**, *200*, 104610. [CrossRef]

31. Singh, J.S.; Gupta, S.R. Plant decomposition and soil respiration in terrestrial ecosystems. *Bot. Rev.* **1977**, *43*, 449–528. [CrossRef]

32. Wang, Z.J.; Yue, F.J.; Xue, L.L.; Wang, Y.C.; Qin, C.Q.; Zeng, J.; Ding, H.; Fu, Y.C.; Li, S.L. Soil nitrogen transformation in different land use and implications for karst soil nitrogen loss controlling. *Catena* **2023**, *225*, 107026. [CrossRef]

33. Tavanti, R.F.R.; Liñares, M.L.; Soares, M.B. Macro-scale spatial modeling reveals the role of soil organic matter quality in CO_2 emissions. *Geoderma Reg.* **2023**, *34*, e00690. [CrossRef]

34. Acosta, M.; Janou, D.; Marek, M.V. Soil surface CO_2 fluxes in a Norway spruce stand. *J. For. Sci.* **2004**, *12*, 573–578. [CrossRef]

35. Batson, J.; Noe, G.B.; Hupp, C.R.; Krauss, K.W.; Rybicki, N.B.; Schenk, E.R. Soil greenhouse gas emissions and carbon budgeting in a short-hydroperiod floodplain wetland. *J. Geophys. Res.-Biogeosci.* **2015**, *120*, 77–95. [CrossRef]

36. Soong, J.L.; Marañon-Jimenez, S.; Cotrufo, M.F.; Boeckx, P.; Bodé, S.; Guenet, B.; Peñuelas, J.; Richter, A.; Stahl, C.; Verbruggen, E.; et al. Soil microbial CNP and respiration responses to organic matter and nutrient additions: Evidence from a tropical soil incubation. *Soil Biol. Biochem.* **2018**, *122*, 141–149. [CrossRef]

37. Al-Omran, A.; Ibrahim, A.; Alharbi, A. Effects of Biochar and Compost on Soil Physical Quality Indices. *Commun. Soil Sci. Plant Anal.* **2021**, *52*, 2482–2499. [CrossRef]

38. Ouyang, Z.; Jackson, R.B.; McNicol, G.; Fluet-Chouinard, E.; Runkle, B.R.; Papale, D.; Knox, S.H.; Cooley, S.; Delwiche, K.B.; Feron, S.; et al. Paddy rice methane emissions across Monsoon Asia. *Remote Sens. Environ.* **2023**, *284*, 113335. [CrossRef]

39. Song, L.N.; Zhang, Y.M.; Hu, C.S.; Zhang, X.Y.; Dong, W.X.; Wang, Y.Y.; Qin, S.P. Comprehensive analysis of emissions and global warming effects of greenhouse gases in winter-wheat fields in the high-yield agro-region of North China Plain. *Chin. J. Eco-Agric.* **2013**, *21*, 297–307. (In Chinese) [CrossRef]

40. Chen, X.P.; Diao, H.J.; Wang, S.P.; Li, H.Y.; Wang, Z.P.; Shen, Y.; Degen, A.A.; Dong, K.H.; Wang, C.H. Plant community mediated methane uptake in response to increasing nitrogen addition level in a saline-alkaline grassland by rhizospheric effects. *Geoderma* **2023**, *429*, 116235. [CrossRef]

41. Bhuiyan, M.S.I.; Rahman, A.; Kim, G.W.; Das, S.; Kim, P.J. Eco-friendly yield-scaled global warming potential assists to determine the right rate of Nitrogen in rice system: A systematic literature review. *Environ. Poll.* **2020**, *271*, 116386. [CrossRef]

42. Shang, Z.H.; Cai, H.J.; Chen, H.; Sun, Y.N.; Li, L.; Zhu, Y.; Wang, X.Y. Effect of Water-Fertilizer-Gas Coupling on Soil N2O Emission and Yield in Greenhouse Tomato. *J. Environ. Sci.* **2018**, *41*, 2924–2935. (In Chinese)

43. Ling, W.; Rong, S.; Yang, H. Stimulatory effect of exogenous nitrate on soil denitrifiers and denitrifying activities in submerged paddy soil. *Geoderma* **2017**, *286*, 64–72.

44. Lei, H.J.; Xiao, Z.Y.; Xiao, R.; Yang, H.G.; Pan, H.W. Effects of water, fertilizer and air coupling drip irrigation on the growth and quality of tomato in greenhouse. *Agric. Res. Arid Areas* **2019**, *38*, 168–175. (In Chinese)

45. Zhang, J.L.; Wang, Z.H.; Chen, X.J. Effects of different nano-bubble irrigation methods and irrigation amount on water consumption and growth of tomato processed by drip irrigation. *Acta Agric. Boreali-occident. Sin.* **2022**, *31*, 1451–1461. (In Chinese)

46. Lei, H.J.; Wang, L.Y.; Pan, H.W.; Hu, S.G. Study on response of growth and nutrient utilization of *Solanum purpurei* to aerated subsurface drip irrigation. *J. Irrig. Eng.* **2019**, *3*, 8–14. (In Chinese)

47. Gao, X.Y.; Yang, J.Q.; Liu, W.Z.; Li, X.Q.; Zhang, W.Z.; Wang, A.J. Effects of alkaline biochar on nitrogen transformation with fertilizer in agricultural soil. *Environ. Res.* **2023**, *233*, 116084. [CrossRef]

48. Ahmad Bhat, S.; Kuriqi, A.; Dar, M.U.D.; Bhat, O.; Sammen, S.S.; Towfiqul Islam, A.R.M.; Elbeltagi, A.; Shah, O.; AI-Ansari, N.; Ali, R.; et al. Application of Biochar for Improving Physical, Chemical, and Hydrological Soil Properties: A Systematic Review. *Sustainability* **2022**, *14*, 11104. [CrossRef]

49. Kang, M.W.; Yibeltal, M.; Kim, Y.H.; Oh, S.J.; Lee, J.C.; Kwon, E.E.; Lee, S.S. Enhancement of soil physical properties and soil water retention with biochar-based soil amendments. *Sci. Total Environ.* **2022**, *836*, 155746. [CrossRef]

50. Lan, Z.; Chen, C.; Rashti, M.R.; Yang, H.; Zhang, D. High pyrolysis temperature biochars reduce nitrogen availability and nitrous oxide emissions from an acid soil. *GCB Bioenergy* **2018**, *10*, 930–945. [CrossRef]

51. Lee, J.H.; Lee, J.G.; Jeong, S.T.; Gwon, H.S.; Kim, G.W. Straw recycling in rice paddy: Trade-off between greenhouse gas emission and soil carbon stock increase. *Soil Tillage Res.* **2020**, *199*, 104598. [CrossRef]

52. Song, H.J.; Lee, J.H.; Canatoy, R.C.; Lee, J.G.; Kim, P.J. Strong mitigation of greenhouse gas emission impact via aerobic short pre-digestion of green manure amended soils during rice cropping. *Sci. Total Environ.* **2020**, *761*, 143193. [CrossRef]

53. Belenguer-Manzanedo, M.; Alcaraz, C.; Camacho, A.; Ibanez, C.; Catala-Forner, M.; Martinez-Eixarch, M. Effect of post-harvest practices on greenhouse gas emissions in rice paddies: Flooding regime and straw management. *Plant Soil* **2022**, *474*, 77–98. [CrossRef]

54. Ennan, Z.; Zhu, Y.; Hu, J.; Xu, T. Effects of Humic Acid Organic Fertilizer on Soil Environment in Black Soil for Paddy Field Under Water Saving Irrigation. *Nat. Environ. Pollut. Technol.* **2022**, *21*, 1243–1249. [CrossRef]

55. Lam, S.K.; Suter, H.; Mosier, A.R.; Chen, D. Using nitrification inhibitors to mitigate agricultural N$_2$O emission: A double-edged sword. *Glob. Change Biol.* **2017**, *23*, 485–489. [CrossRef]

56. Kang, S.Z. Water security and food security. *Chin. J. Eco-Agric.* **2014**, *22*, 880–885. (In Chinese)

57. Yin, F.H. Development status and application prospect of water-saving agriculture and drip irrigation water-fertilizer integration technology. *Chin. Agric. Res.* **2018**, *6*, 30–32. (In Chinese)

58. Lei, H.; Yu, J.; Zang, M.; Pan, H.; Liu, X.; Zhang, Z.; Du, J. Effects of Water-Fertilizer-Air-Coupling Drip Irrigation on Soil Health Status: Soil Aeration, Enzyme Activities and Microbial Biomass. *Agronomy* **2022**, *12*, 2674. [CrossRef]